Results of the Fifth International Spectroradiometer Comparison for Improved Solar Spectral Irradiance Measurements and Related Impact on Reference Solar Cell Calibration

Roberto Galleano, Willem Zaaiman, Diego Alonso-Álvarez, Alessandro Minuto, Nicoletta Ferretti, Raffaele Fucci, Mauro Pravettoni, Martin Halwachs, Matthias Friederichs, Fabian Plag, Dirk Friedrich, and Erik Haverkamp

***Abstract*—This paper reports on the results of the fifth spectral irradiance measurement intercomparison and the impact these results have on the spread of spectral mismatch calculations in the outdoor characterization of reference solar cell and photovoltaic (PV) devices. Ten laboratories and commercial partners with their own instruments were involved in the comparison. Solar spectral irradiance in clear sky condition was measured with both fast fixed and slow rotating grating spectroradiometers. This paper describes the intercomparison campaign, describes different statistical analysis used on acquired data, reports on the results, and analyzes the impact these results would have on the primary calibration of a c-Si PV reference cell under natural sunlight.**

***Index Terms*—Intercomparison, irradiance, solar cell calibration, solar simulator.**

I. Introduction

THE wider portfolio of today's available photovoltaic (PV) technologies on the market makes the measurement of the spectral content of the natural or simulated sunlight a key parameter for the characterization, calibration, and energy yield estimation of these devices. Nowadays, spectroradiometers with different principles of operation (e.g., single- and double-stage rotating grating monochromator or fixed single-grating polychromator with photodiode, PD, array or charge-coupled device, CCD, detectors) are routinely used for solar spectral irradiance measurements. At present, there is a growing request for harmonization of good measurement practices and for knowledge transfer in the field of spectrally resolved solar radiation for solar energy applications (e.g., PVs) in order to make these measurements comparable and directly traceable to the Système international d'unités (SI units). Moreover, periodical round robin or intercomparisons are part of performance-based quality-control checks for laboratories working according to ISO-IEC 17025 [1] standard.

Within this context, a group of European research institutes active in the PV field for research, characterization, and engineering, set up the fifth comparison of spectroradiometers for solar spectral irradiance measurements. Aims of the intercomparison were to assess laboratory measurement capabilities, to exchange and compare instrument calibration procedures, to establish equivalence figures for the measurement of solar spectra, to put in practice lessons learnt from previous editions, and to evaluate the impact the comparison results may have on a practical case. This paper describes the intercomparison campaign, reports on the results, and analyzes the impact these results would have on the primary calibration of a c-Si PV reference cell under natural sunlight.

II. Purpose of the Work—Experimental Approach

There is a growing request for harmonized, traceable, and low-uncertainty solar spectrum measurements for calibration and energy yield estimation in PV. This intercomparison was designed to raise the awareness and exchange good practices on reliable traceable measurements of the solar spectral irradiance with low uncertainty. Moreover, for the participating institutes applying a quality system or having an accreditation according to the ISO/IEC17025 standard [1], the comparison is an implementation, together with round robin, of the required checks for establishing a performance-based quality control system. The intercomparison took place for the second time at the "Instituto

Manuscript received May 13, 2016; revised August 30, 2016; accepted August 31, 2016. Date of publication September 26, 2016; date of current version October 19, 2016. This work was supported in part by the SolCell Project through EMRP Contract ENG51-REG3 and by the project PhotoClass through Contract EMRP ENG55. The EMRP is jointly supported by the European Union and the EMRP participating countries within EURAMET.

R. Galleano and W. Zaaiman are with the Renewables and Energy Efficiency Unit, European Commission DG JRC IET, 21027 Ispra, Italy (e-mail: roberto.galleano@ec.europa.eu; willem.zaaiman@jrc.ec.europa.eu).

D. Alonso-Álvarez is with the Department of Physics, Imperial College London, London SW7 2AZ, U.K. (e-mail: d.alonso-alvarez@imperial.ac.uk).

A. Minuto is with Ricerca sul Sistema Energetico SpA, 20134 Milano, Italy (e-mail: Alessandro.Minuto@rse-web.it).

N. Ferretti is with Photovoltaik Institut Berlin, 10997 Berlin Germany (e-mail: ferretti@pi-berlin.com).

R. Fucci is with ENEA Agenzia Nazionale per Le Nuove Tecnologie l'Energia e lo Sviluppo Economico Sostenibile, 80025 Napoli, Italy (e-mail: raffaele.fucci@enea.it).

M. Pravettoni is with the Institute of Applied Sustainability to the Built Environment, University of Applied Sciences and Arts of Southern Switzerland, CH-6952 Canobbio, Switzerland (e-mail: mauro.pravettoni@supsi.ch).

M. Halwachs is with Austrian Institute of Technology GmbH, 1210 Vienna, Austria (e-mail: Martin.Halwachs@ait.ac.at).

M. Friederichs is with PV Lab Germany GmbH, 14482 Potsdam Germany (e-mail: m.Friederichs@pv-lab.de).

F. Plag and D. Friedrich are with Physikalisch-Technische Bundesanstalt, 38116 Braunschweig, Germany (e-mail: fabian.plag@ptb.de; dirk.friedrich@ptb.de).

E. Haverkamp is with Radboud Universiteit Nijmegen, 6525 HP Nijmegen, Netherlands (e-mail: erik.haverkamp@science.ru.nl).

Color versions of one or more of the figures in this paper are available online at http://ieeexplore.ieee.org.

Digital Object Identifier 10.1109/JPHOTOV.2016.2606698

TABLE I
SUMMARY OF THE CHARACTERISTICS OF THE SPECTRORADIOMETERS INVOLVED IN THE INTERCOMPARISON

Laboratory	Instrument name	Instrument type	Wavelength band (nm)	Calibration & traceability path
AIT	Ocean Optics	Polychromator, two CCD array detector	300–1600	In house, standard lamp
ENEA	Stellarnet	Polychromator, two CCD array detectors	300–1700	External accredited cal. lab.
Imperial College	Ocean Optics HR4000	Polychromator, CCD array detector	250–1100	In house calibration
JRC	OL750	monochromator double PD detector	250–2500	In house, standard lamp
PI Berlin	Tec5	Polychromator, CCD array detector	300–1700	In house, standard lamp
PTB	Instrument System CAS 140CT 156-171	Polychromator, three CCD array detectors	250–2150	In house, standard lamp
RSE	Stellarnet EPP2000	Polychromator, two CCD array detectors	300–1700	Outdoor, AM1.5
Radboud University	EKO MS711	Polychromator, CCD array detector	300–1100	Manufacturer
PV Lab	Instrument System CAS 140CT 156	Polychromator, CCD array detector	300–1100	Manufacturer
SUPSI	EKO wiser system	Polychromator, two CCD array detectors	300–1700	In house, standard lamp

Commercial name, principle of operation, measuring wavelength band, and calibration methods are reported.

Nacional de Técnica Aeroespacial" laboratory, near Madrid, Spain, from May 18–22, 2015. Twelve spectroradiometers systems from six different manufacturers and covering two different technologies (single-stage rotating-grating and fast fixed grating polychromator with single PD or CCD array detectors) were set to simultaneously measure the global normal incidence (GNI) spectral irradiance of natural sunlight from 300 to 1700 nm or 300 to 1100 nm, depending on the available instruments.

A large variety of manufacturers and principles of operation represent a good cross section of today's most used spectroradiometers in the PV community. A selected number of instruments, equipped with suitable collimation tubes to reduce their angle of view [2], were set to measure the direct normal incidence spectral irradiance in the range from 300 to 1700 nm as well. In this paper, only the GNI measurement results from the ten laboratories successfully measuring will be reported.

Due to the technical differences among various instruments in the measurement timing, bandwidth, and spectral resolution, specific procedures for data acquisition, synchronization, and analysis were developed in order to make the spectroradiometers' output data comparable with each other. Data-processing procedures are summarized below and described in more detail elsewhere [3], [4].

Prior to the intercomparison, each participating laboratory calibrated their own spectroradiometer(s) following their usual procedures, thus allowing evaluating the instrument performance together with its traceability chain and calibration procedure. Some spectroradiometers were calibrated by an external accredited calibration laboratory, while others were calibrated in-house using a calibrated radiometric standard lamp or at the manufacturer.

Table I summarizes the main characteristics of the instrument involved: commercial name, instrument type (poly- or monochromator, and detector configuration), the wavelength range covered, and the calibration source. All participating instruments were mounted on high accuracy, 0.5° peak to peak (pk-pk), solar trackers in order to reduce errors due to instruments pointing (e.g., different cosine response of the instruments' entrance optic). In parallel to the intercomparison, a set of cavity radiometers were used as reference detectors for total irradiance data. These last ensure the direct link of solar irradiance measures to the SI units, as these cavity radiometers take part to the international pyrheliometer comparison under the aegis of the World Radiometric Reference, which held every five years at PMOD-Davos, Switzerland [5].

In order to compare solar spectra acquired by "fast" and "slow" measuring instruments, several sets of average spectra, measured during 7-min acquisition time series, were analyzed. The duration of the time series was determined by the acquisition time of the slowest spectroradiometer. During each time series, the irradiance must remain stable to 1%, or better, to consider the series "stable" and flagged for analysis. The stability constraint avoids adding errors arising from fast changing weather or air mass conditions affecting the output of spectroradiometers in different ways. For instance, a cloud rapidly passing close to the sun disk may affect and invalidate only few spectra in the 7-min series acquired by a fast spectroradiometer, whereas for slow spectroradiometers, it may result in a spectrum shape distortion and invalidate the whole 7-min measurement series. This constraint limited the useful sky conditions to clear or almost clear and discarded acquisitions at early morning and late afternoon. Moreover, the acquired spectra were also convoluted using a Gaussian function in order to increase and harmonize the spectral bandwidth to 4-nm full-width half-maximum; this is done to reduce artefacts when comparing spectra in the atmospheric absorption bands [3], [4].

Several analyses were performed on acquired data, both in terms of absolute spectral irradiance and of spectral shape deviations. As described later, diversified data analysis approaches have higher chances of detecting and discriminating errors or uncertainty components due to systematic effects (e.g., instrument calibration) from those arising from instrument nonlinearity, internal stray light or drifts, as some of these errors or uncertainties might not be evident in all analyses.

III. INTERCOMPARISON RESULTS AND DISCUSSIONS

A. Absolute Spectral Irradiance Analysis

Due to a confidentiality nondisclosure agreement among the participants and to avoid commercialism, results will be presented in an anonymous way. Figs. 1–3 show a wavelength-by-wavelength (W-by-W) spectral irradiance deviation analysis performed on a set of typical GNI spectra measured by the partners' instruments over two days of intercomparison. Spectra

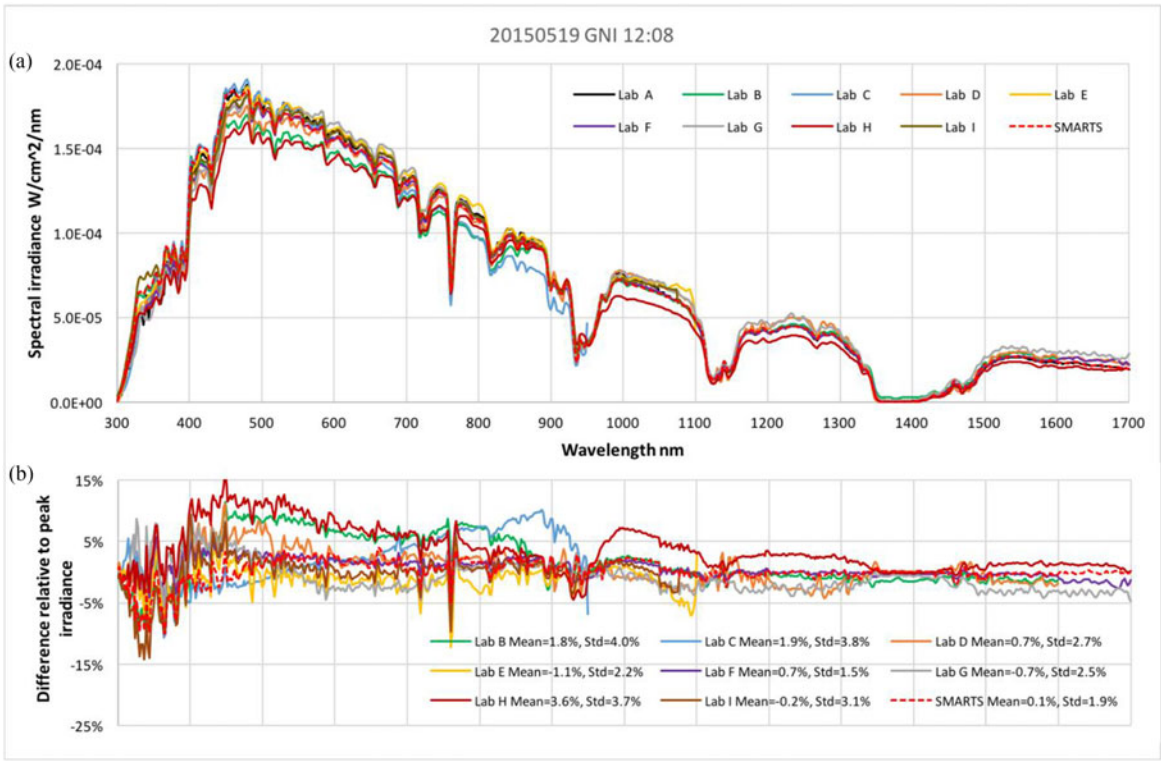

Fig. 1. (a) Nine GNI solar spectra simultaneously measured by participating spectroradiometer systems. (b) W-by-W difference of the Lab A spectrum with respect to spectra measured by other laboratories and normalized to Lab A peak value; calculated average differences and standard deviations are also reported. For comparison purposes, calculated SMARTS spectrum is also added.

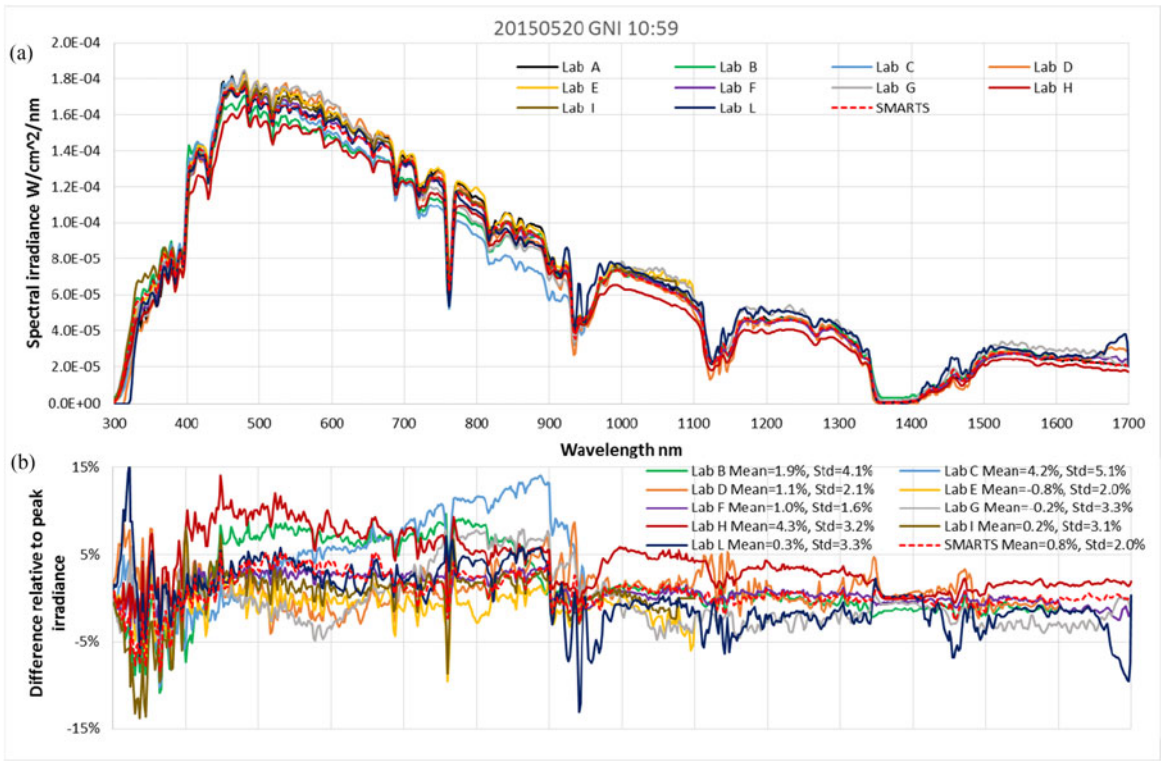

Fig. 2. (a) Ten GNI solar spectra simultaneously measured by participating spectroradiometer systems. (b) W-by-W difference of the Lab A spectrum with respect to spectra measured by other laboratories and normalized to Lab A peak irradiance; calculated mean differences and standard deviations are also reported. For comparison purposes, calculated SMARTS spectrum is also added.

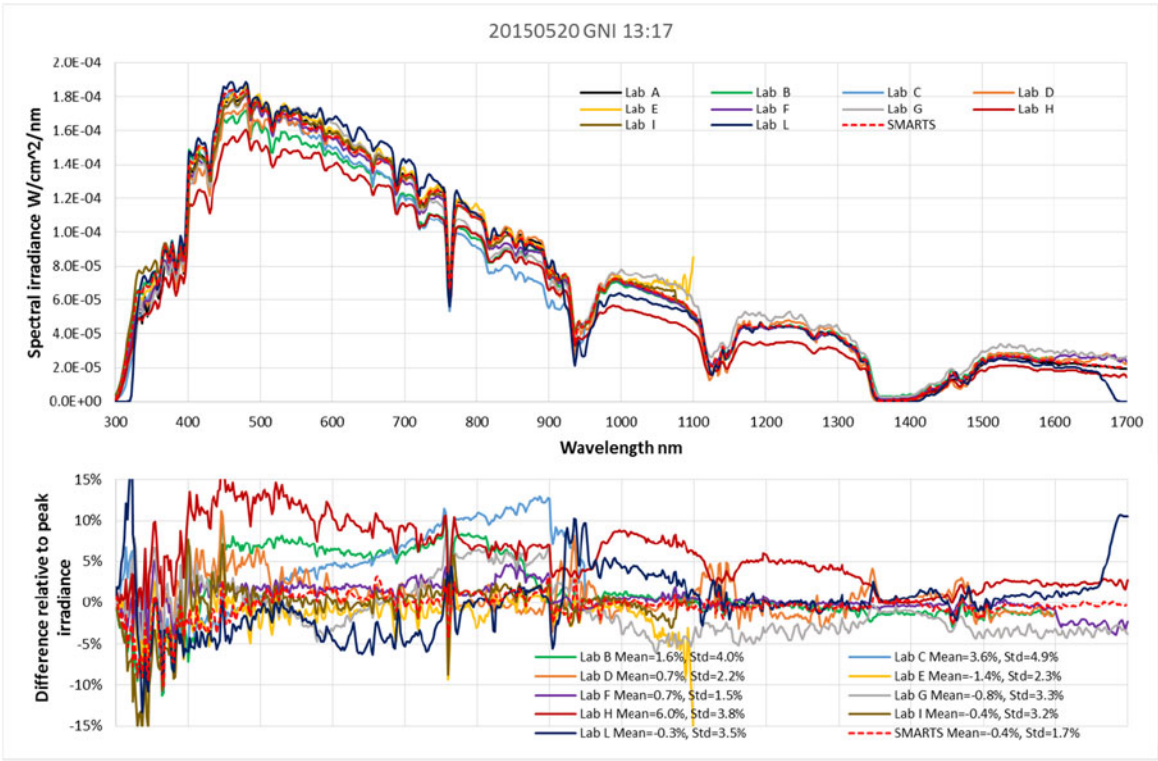

Fig. 3. (a) Ten GNI solar spectra simultaneously measured by participating spectroradiometer systems. (b) W-by-W difference of the Lab A spectrum with respect to spectra measured by other laboratories and normalized to Lab A peak irradiance; calculated mean differences and standard deviations are also reported. For comparison purposes, calculated SMARTS spectrum is also added.

calculated by the Simple Model of the Atmospheric Radiative Transfer of Sunshine (SMARTS) [16] are also included for redundancy and independent check purposes (see Appendix A for details on its use and required inputs).

The graphs in the three figures denoted by letter (a) show a group of stable simultaneously acquired spectra during a 7-min acquisition series. Graphs (b) in the same figures show the W-by-W percent deviation of each spectrum with respect to Lab A spectrum and normalized to its peak irradiance. The Lab A instrument was chosen as reference because it was one of the instruments calibrated via a metrological unbroken chain to the SI units with low uncertainty, and a full evaluation of its calibration uncertainty was provided. W-by-W percent deviation data allow inferring some preliminary information about instrument stability during some hours of continuous outdoor measurements and about instrument reproducibility when considering different days of measurement. All but one instruments were dismounted from trackers at the end of each day and sheltered in a nearby laboratory during the night because they were not specifically designed for permanent outdoor operation.

When considering the entire ensemble of the spectroradiometers, the average W-by-W deviation values for the reported spectra lie in a band of $\pm 2.4\%$ with associated standard deviations up to 4% for Fig. 1, in a band of $\pm 2.6\%$ with associated standard deviations up to 5.1% for Fig. 2, and in a band of $\pm 3.4\%$ with associated standard deviations up to 4.9% for Fig. 3. When considering the behavior of each single instrument shown in Figs. 1–3, most of the instruments achieved repeatable (i.e., during the same day) and reproducible (i.e., during different days) deviations to within 0.6% pk–pk (Labs B, D, E, F, G, and I), two instruments (Labs C and H) showed deviations to within 2.5% pk–pk, and one instrument (Lab L) showed a repeatability to within 0.6% pk–pk during one day of measurement.

While data in Figs. 1–3 show W-by-W mean values calculated on three single acquisitions, a further analysis can be made on the daily average of the W-by-W deviations calculated using all the stable spectra acquired during two days of the comparison. Table II reports the average W-by-W difference values and their standard deviations for the eight stable GNI spectra measured on May 19 and the 21 stable GNI spectra measured on May 20. As to May 19, the average difference values lie within an interval of $\pm 2.7\%$; similar values were found on May 20, where the average difference values lie within an interval of $\pm 3.2\%$. The data labeled as "Lab C recal" are relative to the recalibration exercise described in Section IV. A one-day average standard deviation value much larger than the corresponding one-day average difference denotes a possible instrument intraday drift and/or instability. From an accurate analysis of this information collected all along the comparison campaign, participants can gain knowledge about their instruments' behavior such as temperature stability, repeatability, and reproducibility.

B. *Relative Spectral Irradiance Analysis*

The previous section focused on the absolute spectral irradiance differences among participating instruments; a different

TABLE II
ONE-DAY AVERAGE W-BY-W DIFFERENCES AND STANDARD DEVIATION VALUES CALCULATED WITH RESPECT TO LAB A SPECTRAL IRRADIANCE AND EXPRESSED IN PERCENTAGE OF ITS PEAK IRRADIANCE

	19/05/2015		20/05/2015	
Laboratory	1-day Average difference	1-day average std. dev	1-day Average difference	1-day average std. dev.
Lab B	1.9%	4.1%	1.8%	4.0%
Lab C	3.4%	4.2%	3.9%	5.0%
Lab D	1.8%	2.6%	0.8%	2.1%
Lab E	–0.6%	2.2%	–1.2%	2.0%
Lab F	0.9%	1.5%	0.8%	1.4%
Lab G	–0.7%	2.4%	–0.4%	3.4%
Lab H	4.7%	4.1%	5.1%	3.7%
Lab I	1.1%	3.3%	–0.3%	3.1%
Lab L			–0.2%	3.3%
Lab C recal.	0.1%	1.1%	0.5%	0.6%

Reported data refer to two groups of eight and twenty one stable spectra acquired during 7-min time series on the 19th and 20th of May, respectively. Results from the recalibration of the Lab C instruments are also reported (see Section IV).

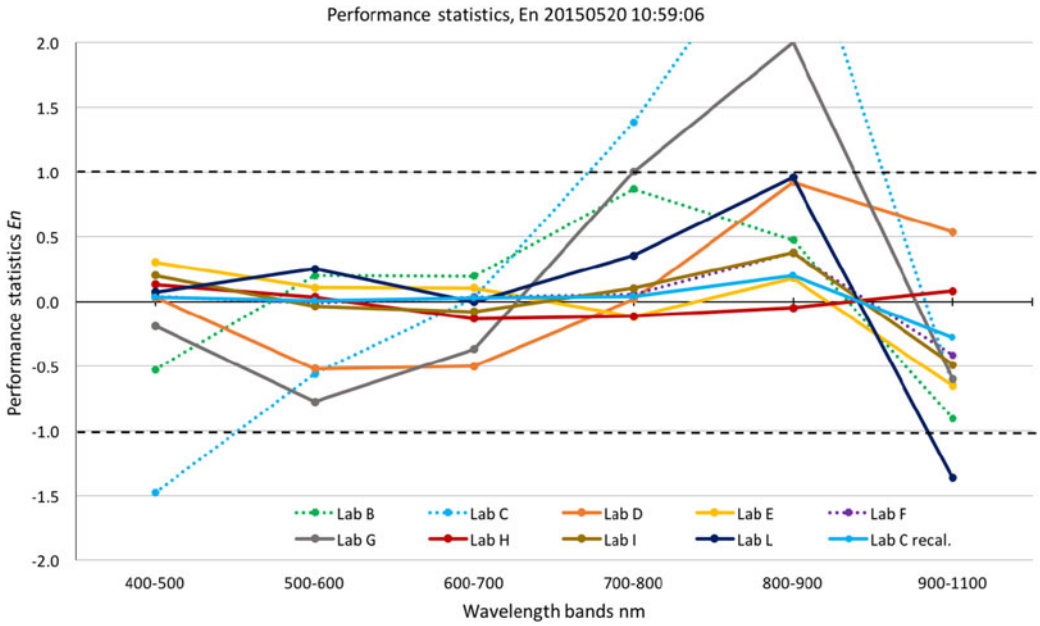

Fig. 4. Performance statistics results using (1). Percent spectral irradiance contents, as integrated in 100-nm bins from 400 to 900 nm plus a 200-nm bin from 900 to 1100 nm, computed from spectra measured by various partner's instruments, are compared with those of the reference instrument and related to declared/assigned measurement uncertainty. Dashed lines at E_n 1, –1 represent acceptance/consistency limits. Results from the recalibration of the Lab C instruments are also reported (see Section IV).

approach can be used to separate systematic effects (e.g., arising from instrument calibration or from instrument time drift), from nonlinearity or spectra distortion due to intrinsic instrument limitation. This approach is important in solar spectrum measurement applied to PV field, where a correct measurement of the spectral distribution of incoming natural sunlight is fundamental, whereas the absolute irradiance value is usually measured by other means, often with lower uncertainty (e.g., cavity radiometers, reference solar cells, pyrheliometers, or pyranometers).

A straightforward comparison of the relative spectral differences among acquired spectra can be done slightly modifying the performance requirement guidelines described in [8]. In fact, the aforementioned standard prescribes dividing the spectral irradiance data of a generic solar simulator into five 100-nm-width bands from 400 to 900 nm, plus an additional 200-nm-width band from 900 to 1100 nm, computes the integral irradiance in each band, and expresses it as the percent ratio to the total irradiance as integrated in the 400–1100 nm band. The percentage distribution of irradiance in each band is, then, compared with the same distribution calculated for the AM1.5G standard spectrum to assess the solar simulator spectral quality class [7], [8].

In this paper, the spectral irradiance data of a specific measurement were integrated as described before and compared with the same distribution of the Lab A spectrum assumed as reference. As a final step, the E_n performance statistics analysis method (for details, see [9]) was applied to the comparison results in each band. The E_n number is a performance statistics

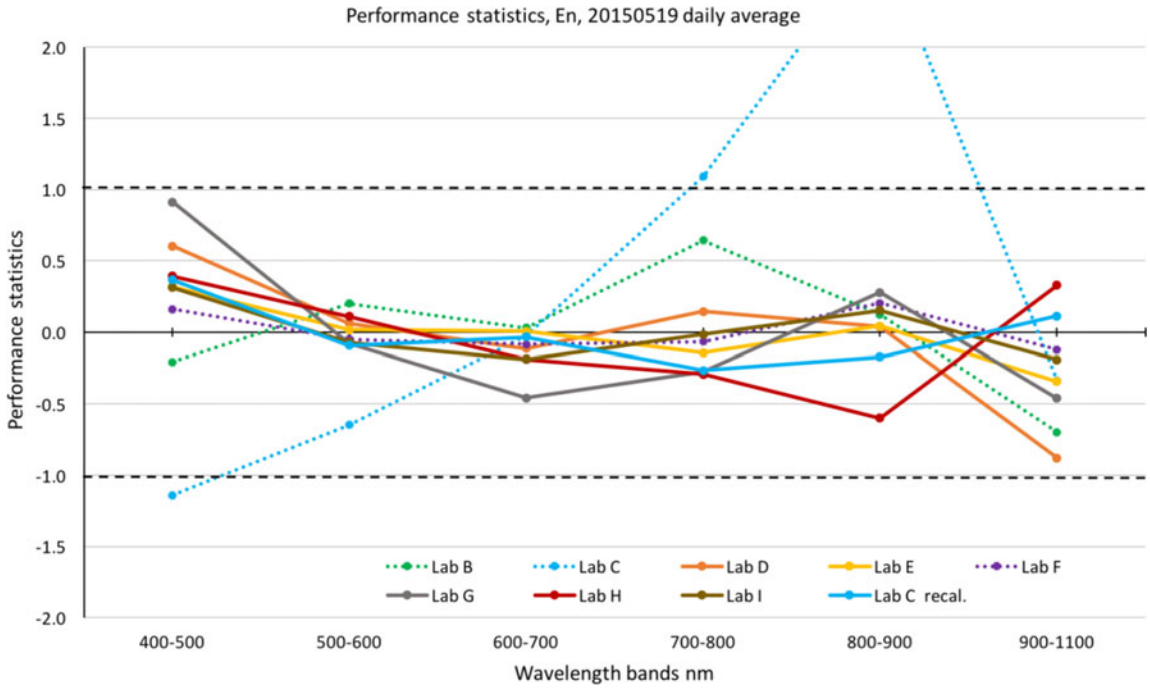

Fig. 5. Average of the performance statistics results using (1) for one-day of stable measurements. Percent spectral irradiance contents, as integrated in 100-nm bins from 400 to 900 nm plus a 200-nm bin from 900 to 1100 nm, computed from spectra measured by various partner's instruments, are compared with those of the reference instrument and related to declared/assigned measurement uncertainty. Dashed lines at E_n 1, –1 represent acceptance/consistency limits. Results from the recalibration of the Lab C instruments are also reported (see Section IV).

tool and is defined as

$$E_n = \frac{M\text{Lab}_i - M\text{ref}}{\sqrt{(U\text{Lab}_i * M\text{Lab}_i)^2 + (U\text{ref} * M\text{ref})^2}} \quad (1)$$

where E_n is the normalized error for the M_{th} band (dimensionless), $U\text{Lab}_i$ and $U\text{ref}$ are the reported expanded ($k = 2$) relative measurement uncertainty for the i_{th} spectroradiometer and the reference, respectively. $M\text{Lab}_i$ and $M\text{ref}$ represent the ratio between the irradiance of the M_{th} band to the total irradiance for the i_{th} spectroradiometer and the reference, respectively.

The calculated E_n number in (1) involves the establishment of acceptance limits of ± 1; E_n values within acceptance limits are considered satisfactory because these are consistent with the estimated uncertainty. E_n values outside acceptance limits highlight inconsistencies with the estimated measurement uncertainty and/or severe instrument drift from the expected performance. For ease of comparison, in this exercise, the expanded relative measurement uncertainty ($k = 2$) was set to a single average value of 5% for $U\text{Lab}_i$ and to 3% for $U\text{ref}$, as resulting from the reference instrument calibration uncertainty.

Fig. 4 shows, as an example, the performance statistics results as applied to the spectra reported in Fig. 2. Six out of nine of the compared instruments show all E_n values within the ± 1 acceptance limits (Labs B, D, E, F, H, and I), two instruments (Labs G and L) show one E_n value outside acceptance limits, and one instrument (Lab C) has severe deviations from the acceptance limits.

It is worth noting that the proposed combined data analysis allowed highlighting that Lab H, despite exhibiting the worst W-by-W average difference in Fig. 2(b), showed E_n values well within consistency threshold, suggesting a systematic effect probably due to a scaling factor in the calibration process. When data from Labs G and L are taken into consideration, an inconsistency in part of their acquired spectra was spotted in the 800–900-nm and 900–1100-nm band, respectively. This result is apparently in contradiction with the low W-by-W average differences shown in Fig. 2(b) by Labs L and G, probably due to the wavy spectra so that the W-by-W differences compensate over the entire wavelength band. The same approach applied to Lab C data confirmed highly divergent results due to instrument nonlinearity or very poor calibration standards or procedures. Lab C recal data are relative to the recalibration exercise described in Section IV.

Extending and applying the performance statistics E_n number analysis to the 28 stable spectra acquired on May 19 and 20, 2015, gives us further information on instruments' time stability.

Figs. 5 and 6 summarize the daily average results; as in the analysis reported in Fig. 4, the ± 1 acceptance limits are set estimating $U\text{Lab}_i$ and $U\text{ref}$ to be 5% and 3%, respectively. Lab C recal data in both figures are relative to the recalibration exercise described in Section IV. The E_n number results do not change very much from one day to another; in both cases, the same instrument systems (Labs B, D, E, F, H, and I) with all deviation values within the acceptance limits (i.e., with deviation values coherent with the estimated uncertainty) reported in Fig. 4 are

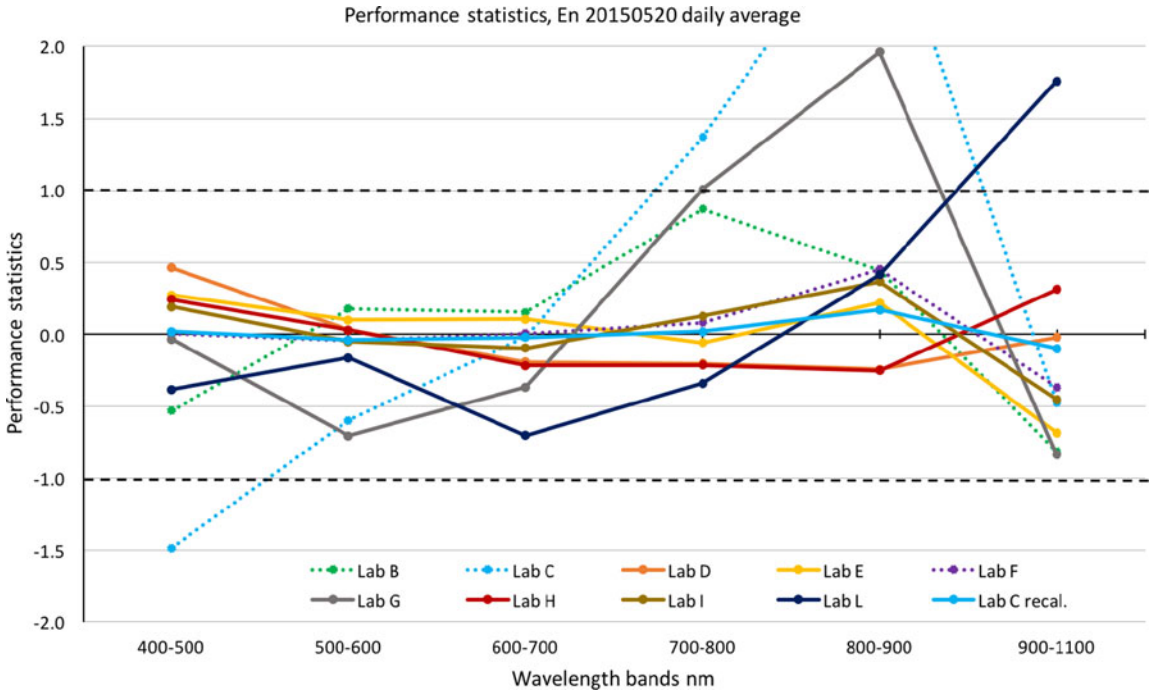

Fig. 6. Average of the performance statistics results using (1) for one-day of stable measurements. Percent spectral irradiance contents, as integrated in 100-nm bins from 400 to 900 nm plus a 200-nm bin from 900 to 1100 nm, computed from spectra measured by various partner's instruments, are compared with those of the reference instrument and related to declared/assigned measurement uncertainty. Dashed lines at E_n 1, –1 represent acceptance/consistency limits. Results from the recalibration of the Lab C instruments are also reported (see Section IV).

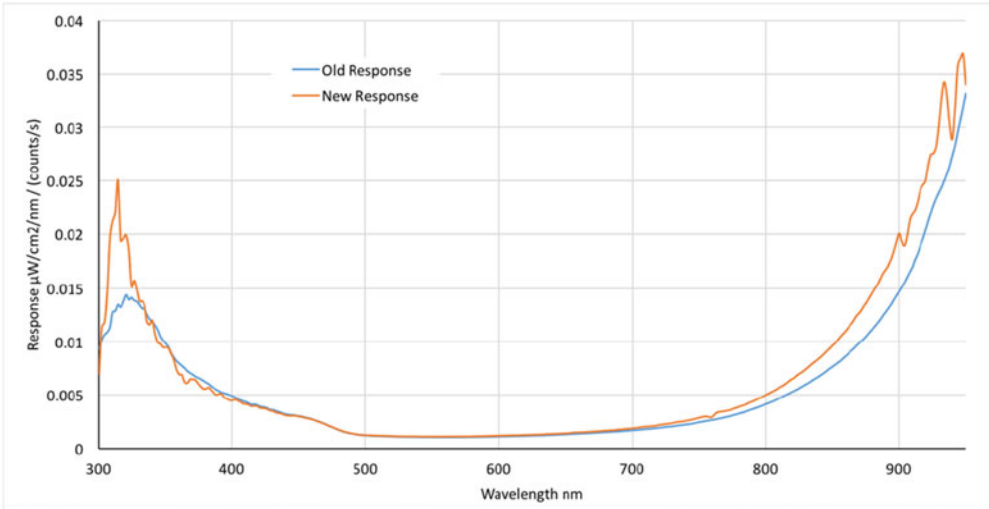

Fig. 7. Old and new calibration curve of the instrument of Lab C after *in-situ* recalibration based on the measurements of Lab A and Lab F on May 20, 2015, at 10:59.

also within ±1 limits in Figs. 5 and 6. This allows assessing the reproducibility of those systems over two days as they were dismounted and sheltered overnight and remounted the day after.

The instrument system belonging to Lab L, which measured only on the 20th, confirmed to have one point (900–1100-nm band) out of the acceptance limits both in a specific measurement of the day and on the daily average, highlighting possible spectroradiometer's misbehavior in the near-infrared wavelength region. In addition, Lab C data confirm severe deviations in three wavelength bands, probably due to inaccurate calibration reference and procedure. Lab G data show a different behavior on the 19th, where its results, shown in Fig. 5, are in accordance with the acceptance levels, compared with the 20th, where the system showed one point out of limits and needs further analysis.

C. Discussion

The large amount of data resulting from the intercomparison must be dealt with diversified analysis methods to extract meaningful information about the characteristics and the

TABLE III
SPECTRAL MISMATCH CORRECTION FACTORS AS COMPUTED USING (3) WITH A SET OF SIMULTANEOUSLY ACQUIRED SOLAR SPECTRA AT DIFFERENT TIME OF THE DAY BY FOUR OF THE SPECTRORADIOMETER SYSTEMS PARTICIPATING TO THE INTERCOMPARISON

	Spectra acquisition time on May 19			
	10:27	*12:08*	*12:18*	*14:47*
MM Lab A	1.003	1.019	1.018	1.018
MM Lab E	1.007	1.021	1.022	1.019
MM Lab F	1.003	1.020	1.020	1.019
MM Lab H	1.004	1.012	1.012	1.011
MM pk–pk % difference	0.4	0.9	1.0	0.8

behavior of the spectroradiometers involved. The complexity of the instruments and measurements requires different analysis approaches trying to separate uncertainty and error components arising from systematic sources (e.g., calibration) from those arising from statistical sources, and those intrinsic to the instrument (e.g., temporal and thermal drift, internal stray light, or grating second-order effect).

In general, a careful scrutiny of the W-by-W deviations calculated from the comparison with simultaneous acquired reference instruments spectra or from, in the case of clear-sky conditions, a modeled SMARTS spectrum may give useful information on the instrument stability at short or long term; if more than one-day data are available, reproducibility information can also be inferred. However, more detailed analysis tools are necessary to better understand the behavior of such complex systems.

In this work, the use of performance statistics tools such as the E_n number allowed us to detect an instrument (Lab H) with good intrinsic performance but with a systematic scaling factor, probably due to calibration (e.g., wrong distance between standard lamp and target spectroradiometer, orientation or misalignment, drift of the reference lamp, etc.).

Moreover, the analysis on selected wavelength bands may give information about instrument behavior on specific wavelength ranges. This is the case for Lab L, exhibiting E_n values within the acceptance limits apart from the near-infrared wavelength band (see Figs. 4 and 6). The same approach applied over two days of measurements gave also a warning about the reproducibility of Lab G instrument that shows all data within the acceptance limits in Fig. 5 but exhibits one point out of the acceptance limits the day after (see Fig. 6).

IV. *In-Situ* CALIBRATION OF SECONDARY INSTRUMENTS

In addition to serve as a comparison of the performance of different instruments, the spectrometer intercomparison could be used to perform an *in-situ* calibration of secondary instruments based on the measurements made by primary instruments with traceability to a standard lamp (e.g., for laboratories not having access to traceable standards). This process is illustrated with the results of Lab C, which showed the poorest performance in terms of spectral distribution measurements (see Section III-B).

The spectra taken on the 20th at 10:59 are used as the recalibration point (see Fig. 2). A new calibration curve for the instrument of Lab C is calculated based on the spectra measured by Labs A and F as

$$R_{\mathrm{New}} = R_{\mathrm{Old}} \frac{G_{\mathrm{Lab}A} + G_{\mathrm{Lab}F}}{2G_{\mathrm{Lab}C}} \tag{2}$$

where R_{New} and R_{Old} are the new and old instrument calibration curves of Lab C, respectively, and $G_{\mathrm{Lab}C}$, $G_{\mathrm{Lab}A}$, and $G_{\mathrm{Lab}F}$ the irradiances measured by Labs C, A, and F, respectively. This equation assumes that the instrument properties—bandpass, slit function, and straylight behavior—are identical for the instruments involved. If that is not the case, the uncertainty of the new calibration curve will be higher. Fig. 7 shows the new calibration curve alongside the old one. As it can be seen, the original calibration was underestimating the solar irradiance in both the short- and long-wavelength bands, while it was comparable in the intermediate band. This trend of having the largest error near the edges of the sensitivity range suggests that the reason for the poor performance of Lab C's instrument might be related to an incorrect account of the background signal of the spectrometer, either during the calibration or during the intercomparison. The ripples in the short- and long-wavelength ranges are an artefact of the recalibration process. They can be related to differences in the instrument bandpass and the convolution and interpolation process described in Section II, which have a large impact in the spectral regions with narrow atmospheric absorption bands. As mentioned, these differences will result in a higher uncertainty of the new calibration curve in these spectral regions.

This new calibration curve is then used to recalculate all spectra measured by Lab C during the intercomparison: the new spectra, duly convoluted and interpolated, have been referred to as "Lab C recal" in the previous sections.

The one-day average W-by-W differences and standard deviations values calculated with respect to Lab A spectra for the measurements of the 19th and 20th are shown in Table II. As can be seen, the recalibration process results in an overall improvement of all the reprocessed measurements compared with Lab A and not only at the calibration point. In particular, the strong reduction of the standard deviation indicates a good stability of the instrument over the time of the intercomparison. The relative spectral distribution analyzed in Section III-B has also improved with the new calibration. In all situations (see Figs. 4–6), Lab C performance statistics have changed from being well outside the ± 1 acceptance limits to less than ± 0.5 in all spectral bands. However, similar performance might not be obtained when measuring light sources with strongly different spectral irradiance distribution due to limitations deriving from different bandpass, slit function, and straylight behavior among involved instruments. This procedure represents, however, an acceptable tradeoff between easy implementation and a higher calibration uncertainty.

This *in-situ* recalibration of secondary instruments not only provides a means of having an instrument calibration curve traceable to a primary instrument: The information can be very valuable for Lab C to identify the critical aspects of their calibration process that need to be revised and improved in order to reach acceptable standards for PV applications.

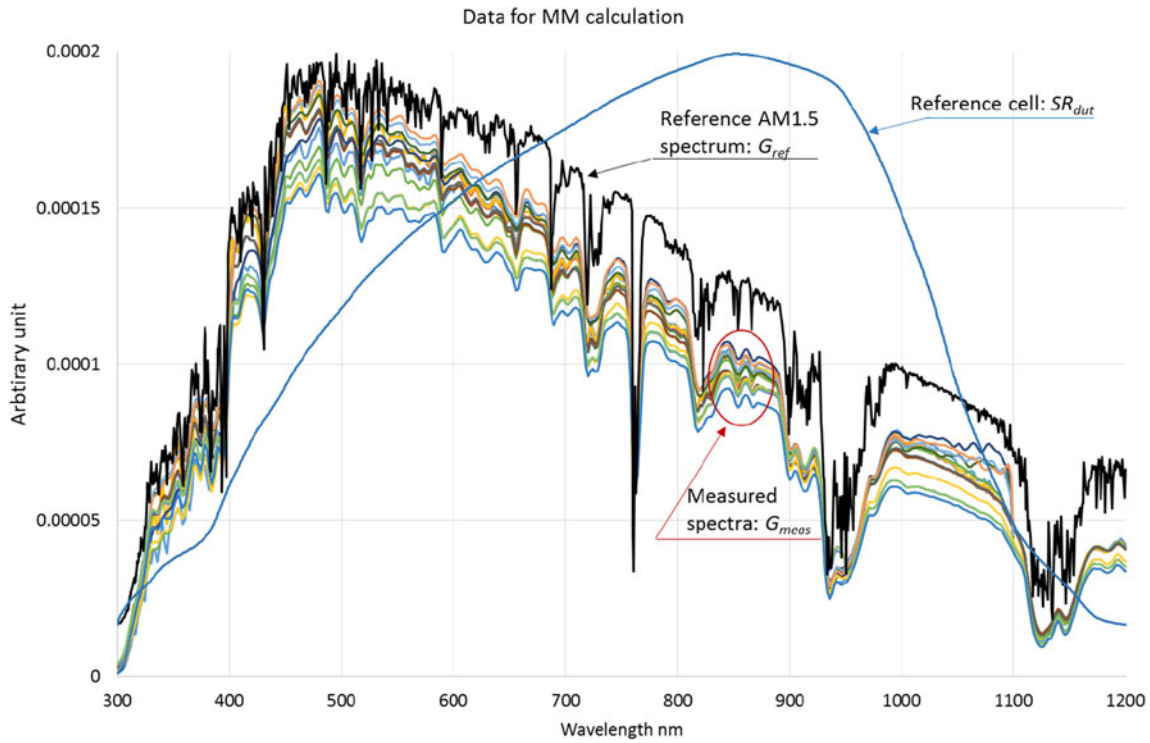

Fig. 8. Reference AM1.5G spectrum $G_{\mathrm{ref}}(\lambda)$ measured spectra at different time of the day by four spectroradiometer systems $G_{\mathrm{meas}}(\lambda)$ and spectral responsivity of calibrating solar cell $SR_{\mathrm{dut}}(\lambda)$ values used in (3) to compute MM values reported in Table III.

V. Results Impact on a Photovoltaic Cell Calibration Exercise

One of the aims of the intercomparison is to establish equivalence confidence limits about the measurements of solar spectrum useful for the PV community. An easy-to-understand way to establish such an equivalence confidence limit is to determine how much the use of solar spectra measured simultaneously by various partners may influence the output of the short-circuit current (I_{sc}) calibration of a reference solar cell.

Several primary calibration methods are described and reported in the annex A of the IEC standard referred to in [10]. Specifically, a slightly modified version of the global sunlight method will be used in the following. The calibration of a PV device at standard test conditions entails, among others, the spectral mismatch correction [6] to the standard spectrum, which is mainly AM1.5G [7] for terrestrial applications. This correction is performed by applying a mismatch correction factor (MM) accounting for the difference in spectral responsivities between the reference device and the testing one, as well as for the relative spectral difference between testing light source and standard spectrum.

The knowledge of the actual spectrum of the solar radiation impinging on the surface of a PV reference cell is one of the necessary parameters for its calibration, the others being the spectral responsivities of the solar cell under calibration and of the reference device used to measure the solar radiation intensity and the AM1.5G reference spectrum. All these input parameters allow computing the following spectral mismatch correction factor

$$\mathrm{MM} = \frac{\int SR_{\mathrm{ref}}(\lambda)\, G_{\mathrm{ref}}(\lambda)\, d\lambda}{\int SR_{\mathrm{ref}}(\lambda)\, G_{\mathrm{meas}}(\lambda)\, d\lambda} \frac{\int SR_{\mathrm{dut}}(\lambda)\, G_{\mathrm{meas}}(\lambda)\, d\lambda}{\int SR_{\mathrm{dut}}(\lambda)\, G_{\mathrm{ref}}(\lambda)\, d\lambda} \tag{3}$$

In (3) $SR_{\mathrm{ref}}(\lambda)$ represents the spectral responsivity of the reference device (which is assumed to be constantly 1 for broadband radiometers), $G_{\mathrm{ref}}(\lambda)$ is the spectral irradiance of the AM1.5G reference spectrum, $SR_{\mathrm{dut}}(\lambda)$ represents the spectral responsivity of the reference solar cell to be calibrated, and $G_{\mathrm{meas}}(\lambda)$ is the actual solar spectrum as measured at the time of calibration.

It is worth noting that MM $= 1$ when $SR_{\mathrm{ref}}(\lambda) = SR_{\mathrm{dut}}(\lambda)$ or $G_{\mathrm{ref}}(\lambda) = G_{\mathrm{meas}}(\lambda)$. Therefore, using a broadband radiometer as a reference device, the deviations between the measured spectrum and the standard AM1.5G are highlighted due to the large spectral responsivity differences between reference device and device under test.

In this exercise, we calculated MM values for different simultaneously measured spectra by four (Labs A, E, F, and H) of the "best-performing" spectroradiometers at different times during the first measurement day (May 15, 2015). According to [10], the integrals of (3) must be computed in the working spectral range of the broadband radiometer used as a reference device (e.g., 250–4000 nm). However, for this exercise, we limited the integrals range from 300 to 1100 nm in order to accommodate the measuring bandwidth of all the involved instruments. Moreover, here, we are interested in highlighting the difference in the

relative spectral shape among the acquired spectra by different partners; hence, the bandwidth reduction will not affect, in the considered wavelength range, the comparison results.

Fig. 8 shows the data used to calculate the MM factors at four different times during a measurement day. It includes the spectral responsivity of the reference cell under calibration, the solar spectra acquired by four spectroradiometers at different times of the day, and the AM1.5G reference spectrum. For display purposes, *Y*-axis arbitrary unit has been chosen in order to shift plots.

MM computation results are reported in Table III. The pk–pk differences of the computed MM ranges from 0.4% for a set of stable simultaneously acquired spectra at the beginning of the measurement day and increases to maximum 1% later during the day, probably due to a slight drift of Lab H instrument.

The MM values for the two reference labs present at the intercomparison (Labs A and F) are in good agreement to within 0.2% pk–pk for the whole measurement day. These results confirm the importance of a correct, reliable, and traceable solar spectrum measurement for high-precision PV device calibration as a 1% difference in the MM factor turns to a 1% difference in the final $I_{\rm sc}$ calibration value.

Although it is possible to reduce the influence of the MM correction factor and, hence, of its uncertainty [11] (e.g., choosing the calibration time and location in order to be as close as possible to AM1.5G condition), it is likely that a significant part of the 1–3% spread reported in the $I_{\rm sc}$ values for PV module [12], [13] and cell [14], [15] calibration round robin is due to the uncertainty in measuring the spectrum of the sun or of the solar simulators.

VI. Conclusion

A spectroradiometer intercomparison was performed among ten European scientific and industrial partners. The intercomparison aimed at exchanging and comparing instrument calibration procedures and measurement capabilities, at establishing equivalence figures for solar spectra measurement, and at putting in practice lessons learnt from previous editions.

A large variety of manufacturers and principles of operation of the instruments involved in the intercomparison are a good cross section of today's most used spectroradiometers in the PV community. Different and complementary data analyses were applied to the measured spectra so that partners can have comprehensive knowledge about their instrument's behavior, calibration, and measurement procedures. The analyses of the results showed W-by-W average differences lying within an interval of $\pm 3.2\%$ for two whole days of measurement, for a total of 28 stable spectra. Performance statistics E_n number analysis applied to the same acquisition days showed that in all the considered wavelength bands, six spectroradiometers have their output consistent with declared measurement uncertainty on both days. One had E_n results consistent with the declared uncertainty on one day and showed partial inconsistency on the other day. One other system showed larger deviation from ± 1 acceptance limits on both days.

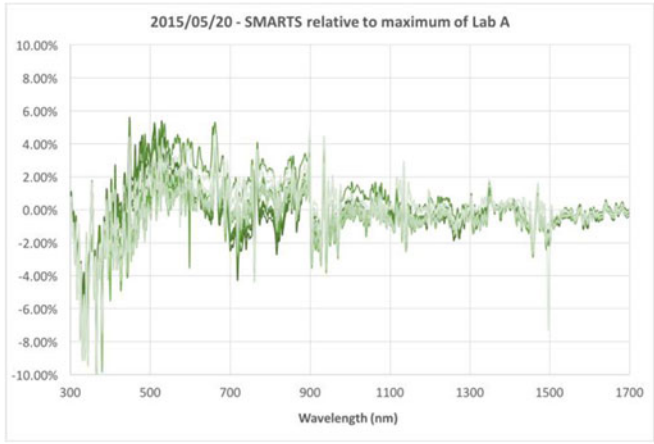

Fig. 9. W-by-W difference of SMARTS synthetic spectra with respect to Lab A for all spectra measured on the May 20, 2015 (21 in total).

Absolute and relative spectral irradiance comparison methodologies proved to be a good approach to separate instrument nonlinearity and distortion effects from systematic effects due to calibration or due to drift with time and/or temperature. In addition to serve as a comparison of the performance of different instruments, the spectrometer intercomparison can be used to perform an *in-situ* calibration of secondary instruments for measuring natural sunlight based on the measurements made by primary instruments with traceability to a standard lamp. Such an exercise proved that correcting acquired spectra according to recalibration significantly improved the agreement with reference instruments and can be valuable for identifying critical aspect of calibration.

When quantifying the impact of using different simultaneously acquired spectra on the $I_{\rm sc}$ calibration of a PV reference cell, we found a maximum 1% pk–pk figure for spectral mismatch calculation using data from four different laboratories, reducing to 0.2% pk–pk when data from two reference laboratories were considered.

Appendix A

SMARTS is used to create synthetic spectra for all the days and times of the intercomparison [16]. Real-time atmospheric parameters (ambient temperature, surface pressure, precipitable water, and humidity) were measured on site or retrieved from public repositories of atmospheric data measured at a weather station in the nearby Madrid-Barajas airport [17]–[19]. Other parameters needed for the simulation (such as albedo or aerosol model) were fixed throughout all simulations. In Appendix B, there is an example of a SMARTS input file for the 9:17 measurement of the May 20, 2015.

Fig. 9 shows the W-by-W difference of SMARTS synthetic spectra with respect to Lab A for all spectra measured on the May 20, (21 in total). A consistent difference less than 5% at all wavelengths and less than 2% for the near-infrared region ($>$900 nm) can be observed independently of the spectrum. These values are on the same order, or better than those obtained experimentally by some of the labs shown in Fig. 1.

APPENDIX B

Example of input file for SMARTS: See SMARTS documentation for a full explanation of the meaning of each "Card" entry.

```
'2015-05-20_09-17_SMARTS' !Card 1
1 !Card 2
952.6 0.625 0.0 !Card 2a
1 !Card 3
'USSA' !Card 3a
0 !Card 4
0.6984846907675195 !Card 4a
1 !Card 5
0 !Card 6
2 !Card 6a
370 !Card 7
0 !Card 7a
'S&F_RURAL' !Card 8
0 !Card 9
0.085 !Card 9a
9 !Card 10
1 !Card 10b
9 -999 -999 !Card 10c
280 4004 1 1367 !Card 11
2 !Card 12
280 4004 0.5 !Card 12a
4 !Card 12b
6, 7, 8, 9 !Card 12c
1 !Card 13
1 2.5 4 !Card 13a
1 !Card 14
1 1700 1700 2 4 !Card 14a
0 !Card 15
0 !Card 16
3 !Card 17
2015 5 20 8.225 40.4966 -3.462 0 !Card 17a
```

REFERENCES

[1] *General Requirements for the Competence of Testing and Calibration Laboratories*, International Organization for Standardization, ISO Central Secretariat, Geneva, Switzerland, ISO/IEC 17025:2005.

[2] *Guide to Meteorological Instruments and Observations*, WMO-No-8 Secretariat of the World Meteorological Org., Geneva, Switzerland, 2006.

[3] R. Galleano *et al.*, "Intercomparison campaign of spectroradiometers for a correct estimation of solar spectral irradiance: Results and potential impact on photovoltaic devices calibration," *Prog. Photovoltaics, Res. Appl.*, vol. 22, pp. 1128–1137, 2014, doi: 10.1002/pip.2361.

[4] R. Galleano *et al.*, "Second international spectroradiometer intercomparison: Results and impact on PV device calibration," *Prog. Photovoltaics, Res. Appl.*, vol. 23, pp. 929–938, 2015, doi: 10.1002/pip.2511.

[5] W. Finsterle, WMO International Pyrheliometer Comparison IPC-XI Final Report, WMO IOM Rep. No. 108, 2011.

[6] *Photovoltaic Devices—Part 7: Computation of Spectral Mismatch Error Introduced in the Testing of a Photovoltaic Device*, International Organization for Standardization, ISO Central Secretariat, Geneva, Switzerland, JISO/IEC 60904-7, 2008.

[7] *Photovoltaic Devices—Part 3 Measurement Principles for Terrestrial Photovoltaic (PV) Solar Devices with Reference Spectral Irradiance Data*, International Organization for Standardization, ISO Central Secretariat, Geneva, Switzerland, ISO/IEC 60904-3, 2008.

[8] *Photovoltaic Devices—Part 9: Solar Simulator Performance Requirements*, International Organization for Standardization, ISO Central Secretariat, Geneva, Switzerland, ISO/IEC 60904-9:2007.

[9] *Conformity Assessment—General Requirements for Proficiency Testing*, ISO Central Secretariat, Geneva, Switzerland, J ISO/IEC 17043:2010.

[10] *Photovoltaic Devices—Part 4: Reference Solar Devices—Procedures for Establishing Calibration Traceability*, International Organization for Standardization, ISO Central Secretariat, Geneva, Switzerland, ISO/IEC 60904-4, 2009.

[11] H. Field and K. A. Emery, "An uncertainty analysis of the spectral correction factor," in *Proc. 23rd IEEE Photovoltaic Spec. Conf.*, 1993, pp. 1180–1187.

[12] Y. Hishikawa *et al.*, "Round-robin measurement intercomparison of c-Si PV modules among Asian testing laboratories," *Prog. Photovoltaics, Res. Appl.*, vol. 21, pp. 1181–1188, 2013, doi: 10.1002/pip.2255.

[13] D. Dirnberger *et al.*, "Progress in photovoltaic module calibration: Results of a worldwide intercomparison between four reference laboratories," *Meas. Sci. Technol.*, vol. 25, 2014, Art. no. 105005, doi: 10.1088/0957-0233/25/10/105005.

[14] P. Manshanden *et al.*, "Round robins of solar cells to evaluate measurement systems of different European Research Institutes," in *Proc. 28th Eur. Photovoltaic Sol. Energy Conf. Exhib.*, Paris, France, Sep. 30–Oct. 4, 2013, pp. 861–866.

[15] H. Müllejans *et al.*, "Reduction of uncertainties for photovoltaic reference cells," *Metrologia*, vol. 52, 2015, Art. no. 646, doi: 10.1088/0026-1394/52/5/646.

[16] SMARTS webpage. Software and User Manual. [Online]. Available: http://www.nrel.gov/rredc/smarts/. Accessed: Jan. 2016.

[17] G. Martinez Fuente, Ambient temperature and humidity measured in-situ at INTA, Private communication.

[18] Atmospheric pressure measured at Madrid-Barajas airport. [Online]. Available: www.ogimet.com, accessed Sep. 2016.

[19] Precipitable water obtained from the Madrid site of AERONET. [Online]. Available: http://aeronet.gsfc.nasa.gov, accessed Sep. 2016.

Authors' photographs and biographies not available at the time of publication.